bjh research paper

Deficient RPS19 protein production induces cell cycle arrest in erythroid progenitor cells

Madoka Kuramitsu, Isao Hamaguchi, Mizukami Takuo, Atsuko Masumi, Haruka Momose, Kazuya Takizawa, Masayo Mochizuki, Seishirou Naito and Kazunari Yamaguchi

Department of Safety Research on Blood and Biological Products, National Institute of Infectious Disease, Musashimurayama, Tokyo, Japan

Received 11 July 2007; accepted for publication 28 September 2007

Correspondence: Isao Hamaguchi, Department of Safety Research on Blood and Biological Products, National Institute of Infectious Disease, Gakuen 4-7-1, Musashimurayama, Tokyo 208-0011, Japan. E-mail: 130hama@nih.go.jp

Summary

The gene encoding ribosomal protein S19 (*RPS19*) is one of the responsible genes for Diamond-Blackfan anaemia (DBA), a congenital erythroblastopenia. Although haplo-insufficiency of *RPS19* has been suggested to be the onset mechanism underlying the pathogenesis of DBA, the sequential mechanism has not been elucidated. In order to analyse the consequences of the missense mutation of *RPS19* specific for DBA patients, we made mutated *RPS19* expression vectors. Twelve C-terminally Flag-tagged missense mutants were exogenously expressed from retroviral vectors and analysed by Western blot analysis and flow cytometry. When these 12 mutants were expressed in the erythro-leukaemic cell lines K562 and human bone marrow $CD34^+$ cells, almost all of the mutant proteins (except for G120R) were unstable, and the levels of mutated RPS19 protein were significantly low. To address the effect of deficient *RPS19* expression on cell proliferation, *RPS19* was downregulated by siRNA. Repressive expression of *RPS19* in human $CD34^+$ cells produced an elevated number of cells at G0 and induced erythroid progenitor-specific defects in BM cells. These results suggest that abnormal ribosomal biogenesis causes inadequate cell cycle arrest in haematopoietic progenitors, and that, subsequently, erythroid progenitors are specifically hampered. These *in vitro* phenotypes of genetically manipulated $CD34^+$ cells mimic DBA pathogenesis.

Keywords: Diamond-Blackfan, RPS19, haplo-insufficiency, cell cycle, gene mutation.

Diamond-Blackfan anaemia (DBA) is a congenital severe red blood aplasia with a frequency of 5–7 per million live births, usually presenting during the first year of life (Diamond *et al*, 1976; Willig *et al*, 1999a).

The disease is characterized by severely reduced erythroid precursors in the bone marrow (BM). Approximately 30–40% of patients have associated physical malformations, including prenatal or postnatal growth retardation, craniofacial abnormalities, hand and thumb malformations, and congenital heart defects (Willig *et al*, 2000; Lipton, 2006).

Approximately 25% of patients with DBA have a mutation in one allele of the ribosomal protein S19 gene (*RPS19*) (Draptchinskaia *et al*, 1999; Willig *et al*, 1999b) and 2% have a mutation in one allele of *RPS24* (Gazda *et al*, 2006). Forced expression of RPS19 in the haematopoietic stem cells of DBA patients with an *RPS19* mutation resulted in a recovery of deficient colony formation *in vitro* (Hamaguchi *et al*, 2002). These results suggested that mutated *RPS19* may cause the insufficient expression level of RPS19 for erythroid cell production.

Pathogenic analyses of DBA have been reported. Several expression analyses in patients with *RPS19*-mutated DBA have confirmed that RPS19 expression from the healthy *RPS19* allele is not sufficient to compensate for the abnormal allele (Hamaguchi *et al*, 2002; Gazda *et al*, 2004). Also, when green fluoroscent protein (GFP)-fused RPS19 mutants were transiently expressed in some culture cell lines *in vitro*, several *RPS19* mutations resulted in low level expression (Da Costa *et al*, 2003). A homozygous null mutation in mice (*Rps19−/−*) is embryonic lethal before the formation of blastocysts, although *Rps19+/−* heterozygous mice were reported to have a normal haematocrit, and the *RPS19* mRNA levels appeared

to be similar between *Rps19*+/+ and *Rps19*+/− mice (Matsson *et al*, 2006). Downregulation of *RPS19* by siRNA successfully produced phenotypes similar to DBA (Ebert *et al*, 2005; Flygare *et al*, 2005; Miyake *et al*, 2005). Furthermore, several groups have demonstrated that downregulation of *RPS19* caused a defect in ribosome biogenesis in yeast and human cells that was also observed in cells from DBA patients (Léger-Silvestre *et al*, 2005; Choesmel *et al*, 2007; Flygare *et al*, 2007). However, it remains to be identified whether mutated RPS19 acts as a key molecule in haematopoietic cell differentiation.

As DBA is a rare disease, it is difficult to obtain sufficient patient samples for a thorough analysis. In order to elucidate the functions of mutant RPS19, we performed *in vitro* analysis by using retrovirus and lentivirus gene transduction. We performed expression analyses of *RPS19* missense mutants in K562 cells and primary BM cells, and found that the expression levels of almost all missense mutants in K562 and BM cells were dramatically low, almost at background level. Cells with low RPS19 levels owing to a siRNA against *RPS19* went into cell cycle arrest at the G0/G1 phase. Cell cycle arrest was induced especially in CD71-high, CD45RA negative erythroid progenitor cells.

These results indicated that RPS19 encoded by a mutated allele was produced at a low level, and that this reduced level of RPS19 is an inducer of cell cycle arrest, especially in erythroid progenitors. This arrest may contribute to the defect in erythropoiesis seen in DBA patients.

Experimental procedure

Cells and culture conditions

K562 cells were maintained in RPMI1640 medium containing 10% fetal bovine serum (FBS). BM $CD34^+$ cells were purchased from Sanko Junyaku (Tokyo, Japan) and cultured in the presence of 1% bovine serum albumin (BSA; Stem Cell Technology, Vancouver, BC, Canada), 100 ng/ml stem cell factor (SCF; Peprotech, London, UK), 100 ng/ml thrombopoietin (TPO; a gift from Kirin Brewery, Tokyo, Japan), 100 ng/ml Flt-3 ligand (Peprotech), and 10^{-4} mol/l 2-mercaptoethanol, in X-Vivo 15 (BioWhittaker, Walkersville, MD, USA).

For erythroid liquid culture, $CD34^+$ cells were cultured in Iscove's Modified Dulbecco's Medium (IMDM; Sigma, St Louis, MO, USA) containing 30% FBS, 1% BSA, 10^{-4} mol/l 2-mercaptoethanol, 100 U/ml penicillin-streptomycin and 2 mmol/l L-glutamine with the following cytokines: 10 U/ml erythropoietin, 0·001 ng/ml granulocyte-macrophage colony-stimulating factor and 0·01 U/ml interleukin-3.

Transduction of $CD34^+$ cells

Frozen BM cells were thawed in 0·25 mg/ml *DNase* I (Roche Diagnostics, Mannheim, Germany)-containing medium to avoid clumping of cells. Pre-stimulation of $CD34^+$ cells was performed under serum-free conditions in X-vivo 15 medium (BioWhittaker) supplemented with 1% BSA, 0·2-μm-filtered 2-mercaptoethanol (Sigma), 100 U/ml penicillin-streptomycin, and 2 mmol/l L-glutamine with the following cytokines: 100 ng/ml SCF (Peprotech), 100 ng/ml TPO (a gift from Kirin Brewery) and 100 ng/ml Flt-3 ligand (Peprotech). Transduction was performed according to the manufacturer's instructions. Briefly, retroviruses were loaded onto RetroNectin-coated 96-well dishes, and then incubated at 37°C for 4 h. $CD34^+$ cells were then added to the retrovirus-loaded dish after removal of viral supernatant, and incubated at 37°C in a humidified atmosphere with 5% CO_2.

Construction of RPS19 mutant expression vectors

RPS19 mutants were generated by polymerase chain reaction (PCR) from K562 cDNA, and cloned into pcDNA3.0 at the EcoRI and XhoI sites. The PCR primer pair used was as follows: forward: aggaattccgccatgcctggagttactgta, reverse: tgctcgagtc**acttgtcgtcgtcgtccttgtagtc**gggcccatgcttcttgttgg. The Flag tag sequence is shown in bold. The forward and reverse primer pairs used to generate *RPS19* mutants are described in Table I. All vectors obtained were sequenced to confirm that there are no mutations except for the one point mutation we generated. Transfection was performed by electroporation of 1×10^7 cells with 20 μg of plasmid DNA, in a 4-mm-diameter cuvette, using a Gene Pulser (Bio-Rad, Richmond, CA, USA) at 220 V and 975 μF.

For construction of retrovirus vectors, *RPS19* mutants were cloned into the retrovirus vector pBMN-GFP (Orbigen, San Diego, CA, USA) at the EcoRI and XhoI sites, which are located at the beginning of an internal ribosome entry site (IRES)-GFP cassette.

To obtain retroviral supernatant, retroviral vector was transfected into a Phoenix-Ampho packaging cell line by calcium–phosphate precipitation under standard conditions (Hamaguchi *et al*, 2002). Medium was replaced with fresh medium after 15 h. Retroviral supernatants were harvested 24 h later, filtered through a 0·45-μm pore size filter (Millipore, Bedford, MA, USA), and stored at −80°C before use.

Construction of lentivirus vector

The construction of lentiviral vectors was performed as described previously (Flygare *et al*, 2005). In brief, *RPS19* siRNA A (si-A), *RPS19* siRNA C (si-C), and non-specific control siRNA (scrambled, Scr) oligonucleotides were described previously (Flygare *et al*, 2005). Hybridized oligonucleoties were ligated into the BglII-HindIII sites of the pSuper vector (OligoEngine, Seattle, WA, USA), downstream of the H1 promoter. The H1-hairpin-precursor cassette was excised from pSuper with EcoRI and ClaI and further cloned into the EcoRI-ClaI sites of the pLV-TH plasmid (Wiznerowicz & Trono, 2003). The plasmid pLV-TH was a kind gift from Dr Trono, National Centre for Competence in Research,

Table I. RPS19 missense mutations and PCR primers.

DNA mutation	Amino acid alternation	PCR primers*	References†
43 G→T	V15F	forward: 5′-gcaggagttcTtcagagctctg-3′ reverse: 5′-cagagctctgaAgaactcctgc-3′	b
53 T→G	L18R	forward: 5′-tcagagctcGggcagcc-3′ reverse: 5′-ggctgccCgagctctg-3′	e
140 C→T	P47L	forward: 5′-gagcttgctcTctacgatgaga-3′ reverse: 5′-tctcatcgtagAgagcaagctc-3′	c
154 T→C	W52R	forward: 5′-tacgatgagaacCggttctacac-3′ reverse: 5′-gtgtagaaccGgttctcatcgta-3′	a
167 G→A	R56Q	forward: 5′-acacgcAagctgcttcc-3′ reverse: 5′-agcagctTgcgtgtaga-3′	b, d
176 C→T	S59F	forward: 5′-gagctgcttTcacagcgcg-3′ reverse: 5′-cgcgctgtgAaagcagctc-3′	e
182 C→A	A61Q	forward: 5′-cttccacagAgcggcacct-3′ reverse: 5′-aggtgccgcTctgtggaag-3′	d
184 C→T	R62W	forward: 5′-ccacagcgTggcacctgta-3′ reverse: 5′-ggtgccAcgctgtggaag-3′	a, b, c, d
302 G→A	R101H	forward: 5′-tgtggcccAccgggtcc-3′ reverse: 5′-ggacccggTgggccaca-3′	b
358 G→C	G120R	forward: 5′-aagatggcCgccgcaaa-3′ reverse: 5′-ttgcggcGgccatcttg-3′	b
380 G→A	G127Q	forward: 5′-gacacctcaggAacaaagagatct-3′ reverse: 5′-agatctctttgtTcctgaggtgtc-3′	b
392 T→G	L131R	forward: 5′-caaagagatcGggacagaatcg-3′ reverse: 5′-gattctgtccCgatctctttg-3′	e
Quantitative PCR primers			
ACTB		forward: 5′-gcctgacggccaggtcat-3′ reverse: 5′-caggactccatgcccaggaa-3′	
RPS19		forward: 5′-tggaggggctgaaaatggtg-3′ reverse: 5′-cggcgattctgtccagatctc-3′	
CDKN1A		forward: 5′-agaccagcatgacagatttctacca-3′ reverse: 5′-gaagatgtagagcgggcctttg-3′	
CDKN1C		forward: 5′-gctgcggtgagccaatttagag-3′ reverse: 5′-gccggttgctgctacatgaac-3′	

*Mutations are shown by a capital letter.
†a, Draptchinskaia *et al* (1999); b, Willig *et al* (1999b); c, Ramenghi *et al* (2000); d, Cmejla *et al* (2000); e, Gazda *et al* (2004).

Switzerland. Lentivirus was produced by transient transfection of 293T cells by calcium–phosphate precipitation under standard conditions, as described previously (Flygare *et al*, 2005). Medium was replaced with fresh medium after 15 h. Lentiviral supernatants were harvested 24 h later, filtered through a 0·45-μm pore size filter and concentrated by ultracentrifugation (1·5 h at 25 000 *g* at 4°C). The viral batches were titred on HeLa cells.

Quantitative reverse transcription (RT)-PCR

Total RNA was isolated from about 1×10^6 K562 cells using ISOGEN as described by the manufacturer (Nippongene, Tokyo, Japan), and cDNA was reverse transcribed using Superscript III (Invitrogen, Carlsbad, CA, USA). Total RNA of fluorescence-activated cell sorting (FACS) sorted cells was isolated using NucleoSpin RNA II kit (Macherey-Nagel, Duren, Germany), and cDNA was synthesized using the Super SMART PCR cDNA Synthesis kit (Takara, Tokyo, Japan) according to the manufacturer's protocol. The expression level of *RPS19*, *CDKN1A* and *CDKN1C* mRNA was analysed by quantitative reverse transcription-polymerase chain reaction (Q-PCR) using a LightCycler instrument (Roche Diagnostics). PCR was performed using SYBR PREMIX Ex-Taq as described by the manufacturer (Takara). The primer pairs used for Q-PCR are described in Table I.

Cell cycle analysis

To analyse the cell cycle, cells were fixed in 2% formaldehyde for 30 min at 4°C and then resuspended in 70% ethanol and kept at −20°C for more than 6 h.

For analysis of combined RNA and DNA contents, fixed cells were washed twice with 1% BSA in phosphate-buffered

saline (PBS), resuspended at 0·5–2·0 × 10^5 cells in 300 μl of 2 μg/ml Hoechst33342 and 1% BSA in PBS and incubated for 20 min at 37°C. An equal volume of 3 μg/ml Pyronin Y, 2 μg/ml Hoechst33342 and 1% BSA in PBS was added directly and incubation continued for an additional 20 min.

To analyse the expression of Ki-67 antigen and DNA content, fixed cells were washed twice with 2% BSA in PBS, resuspended at 0·5–2·0 × 10^5 in 500 μl of 2% BSA in PBS and incubated with an anti-Ki-67 antibody (Dako, Glostrup, Denmark) at 1:400 for 2 h at 4°C. Cells were washed twice with 2% BSA in PBS and incubated with phycoerythrin (PE)-conjugated anti-Mouse IgG (eBioscience, San Diego, CA, USA) at 1:400 for 1 h at 4°C. Cells were washed twice with 2% BSA and analysed using a JSAN cell sorter (Bay Biosciences, Kobe, Japan). To detect GFP, Pyronin Y, Hoechst33342 and PE, FL1-H, FL2-A, FL7-A and FL2-A channel were used respectively.

Western blotting

Cells were lysed in 1% sodium dodecyl sulphate (SDS) and sonicated. Protein concentrations were determined using a bicinchoninic acid (BCA) assay kit (Promega Madison, WI, USA). Cell lysates were boiled for 5 min in Laemmli buffer. Total protein (25 μg) was subjected to 12·5% SDS–polyacrylamide gel electrophoresis (SDS-PAGE), then transferred onto a polyvinylidenefluoride membrane (Millipore) for 2 h at a constant current using a Criterion Transblot cell (Bio-Rad, Hercules, CA, USA). The membrane was blocked for 1 h at room temperature in blocking solution (5% non-fat milk, 20 mmol/l Tris pH 7·4, 150 mmol/l NaCl). The membranes were incubated with the following antibodies in antibody buffer (3% non-fat milk, 20 mmol/l Tris pH 7·4, 150 mmol/l NaCl, 0·05% Tween 20) overnight at 4°C: anti-Flag M2 (Sigma) at 1:1500; anti-GFP (MBL, Nagoya, Japan) at 1:1000; anti-Rb [Becton Dickinson (BD), San Diego, CA, USA] at 1:1000; anti-actin (SantaCruz, CA, USA) at 1:1000. Blots were then incubated with horseradish peroxidase (HRP)-conjugated anti-mouse or anti-goat immunoglobulin at a dilution of 1:5000 in antibody buffer, for 1 h at room temperature. Bands of immunoreactive proteins were detected using SuperSignal™ West Dura chemiluminescent substrate (Pierce, Rockford, IL, USA).

Flow cytometry

Cells were fixed with 2% formaldehyde for 30 min at 4°C. Then, cells were fixed with 70% ethanol and stored at −20°C for more than 6 h. Fixed cells were washed twice with 2% BSA/PBS, and blocking was performed with 2% BSA/PBS for 1 h at 4°C. Cells were incubated with 2% BSA/PBS containing anti-Flag M2 (Sigma) at a dilution of 1:2000 for 1 h at 4°C. Then cells were washed twice with 2% BSA/PBS and incubated with anti-mouse IgG1-APC (BD) at a dilution of 1:4000 for 30 min at 4°C. The intensity of APC signal was analysed using a JSAN cell sorter (Bay Bioscience).

Progenitor assay

Cells were washed with PBS, and suspended in FACS medium (3% FBS in PBS). Biotin-conjugated anti-CD71 (eBioscience) was added at a dilution of 1:500 and incubated for 1 h at 4°C. Cells were washed twice with FACS medium and then resuspended in FACS medium containing avidin-APC-Cy7 (eBioscience) and anti-CD45RA-APC (eBioscience) at dilutions of 1:500 and 1:20, respectively, and incubated for another 1 h at 4°C. Cells were washed twice with FACS medium and GFP-positive cells were gated; the intensities of APC-Cy7 (FL6-H) and APC (FL5-H) signals were analysed using a JSAN cell sorter (Bay Bioscience).

Detection of apoptotic cells

Cells were stained with allophycocyanin (APC)-conjugated Annexin-V (BD) and propidium iodide (PI) (BD) according to the manufacturer's protocol, and analysed using a JSAN cell sorter (Bay Bioscience).

Results

One point mutation of RPS19 *caused decreased levels of RPS19 protein*

Many *RPS19* mutations, including missense and non-sense mutations, insertions, deletions and splice site deletions, have been associated with DBA (Draptchinskaia *et al*, 1999; Willig *et al*, 1999b; Cmejla *et al*, 2000; Ramenghi *et al*, 2000; Proust *et al*, 2003; Gazda *et al*, 2004; Orfali *et al*, 2004). Haploinsufficiency is a common anaemic phenotype among these mutations. This study investigated whether DBA-associated various single-point missense mutations also indicated haploinsufficiency. Expression vectors were constructed that contained different single-point mutations in *RPS19* (Table I), as previously reported (Draptchinskaia *et al*, 1999; Willig *et al*, 1999b; Cmejla *et al*, 2000; Ramenghi *et al*, 2000; Gazda *et al*, 2004). In these vector constructs, mutated *RPS19* were fused with a Flag tag sequence at the C-terminus of RPS19 mutants, because the N-terminal methionine of RPS19 was reported to be removed post-transcriptionally (Vladimirov *et al*, 1996).

We transfected K562 cells with these vectors to analyse the expression of mutated *RPS19* at 24 h post-transfection. The levels of RPS19 protein were judged based on the levels of Flag. Western blot analysis using an anti-Flag antibody revealed a dramatic decrease in the levels of almost all mutant proteins, except for G120R, compared with wild-type RPS19 (Fig 1A). These results were confirmed by three separate experiments.

To analyse the transcriptional and translational processes from the mutated RPS19 sequence of the vector, we prepared a bi-cistronic retroviral expression system in which GFP was expressed from an IRES sequence downstream of the mutated *RPS19* cassette (Fig 1B). K562 cells were infected with bi-cistronic retrovirus vectors and fixed at 4 d postinfection.

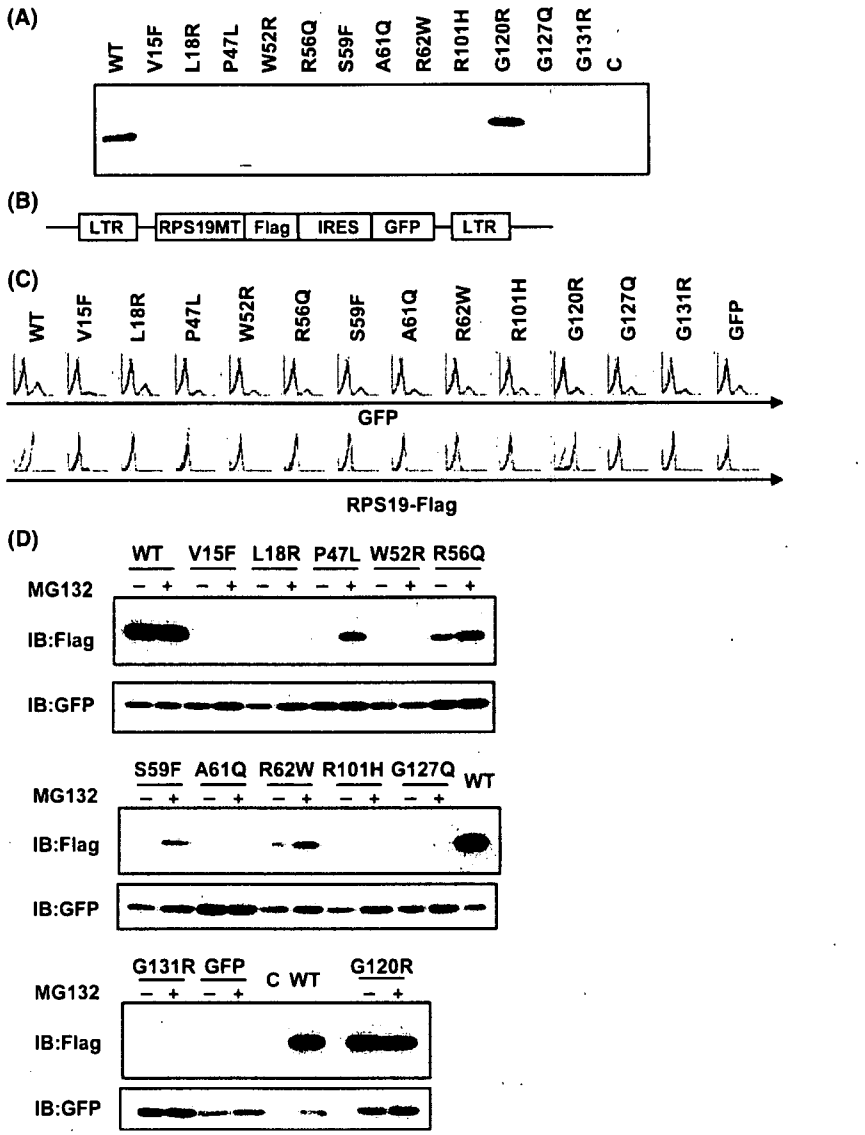

Fig 1. Expression analysis of RPS19 mutants in human erythroleukaemia K562 cells (A) K562 cells were transfected with wild-type *RPS19*, mutant *RPS19* (RPS19mt), or control vector. Cells were lysed and 25 μg of total protein was subjected to Western blot analysis. RPS19-Flag and RPS19mt-Flag were detected using a Flag M2 antibody (WT: wild-type RPS19; C: control empty vector). Data are from one of three experiments with similar results. (B) Construction of the bi-cistronic vector. RPS19 and RPS19mt were inserted in front of the IRES cassette. (C) K562 cells were transduced with retrovirus vector expressing RPS19, RPS19mt or control vector. Cells were fixed and stained with Flag M2 antibody, followed by staining with APC-conjugated anti-mouse IgG. GFP (upper panel) and APC (lower panel) signals were analysed by flow cytometry and are indicated as thick lines. The thin lines indicate the negative controls (upper panel: mock cells; lower panel: GFP-transduced cells) (D) Retrovirus-transduced K562 cells were sorted based on GFP signal. Cells were cultured and treated with DMSO or MG132 at 10 μmol/l for 6 h. Cells were subjected to Western blot analysis with anti-Flag (upper panel) and anti-GFP (lower panel) antibodies. Data are from one of three experiments with similar results.

Both GFP and RPS19-Flag expression were analysed by flow cytometry. In the GFP-positive fraction, the expression of RPS19mt-Flag was detected using the anti-Flag antibody. As shown in Fig 1C, except for G120R, the levels of RPS19 mutant proteins were massively decreased.

In order to analyse the post-translational degradation of mutated RPS19 protein, the proteosome inhibitor MG132 was added to the culture medium of mutated RPS19-expressing K562 cells. The expression of RPS19 was then analysed using the anti-Flag antibody. As shown in Fig 1D, Western blot analysis showed that the levels of some mutated RPS19 proteins (four of 12 mutations) were slightly elevated by the inhibition of proteasomal degradation using MG132.

These results suggest that mutated RPS19 should be translated from the vector sequence, as the GFP gene cassette located downstream of *RPS19* was sufficiently expressed among wild-type RPS19-, mutant RPS19- and control GFP-transduced cells. Thus, the decreased levels of some RPS19 mutants were partially due to post-translational degradation in the proteosome.

Effects of single-point mutations in RPS19 in human haematopoietic stem cells

Next, we tried to elucidate the effects of RPS19 point mutants in primary human $CD34^+$ haematopoietic cells. We infected primary BM $CD34^+$ cells with retrovirus expressing RPS19 mutants fused to a Flag tag sequence at the C terminus. Subsequently, half of the infected cells were cultured in a stem cell-maintaining medium containing SCF, TPO and Flt3-ligand, for 3 d; the other cells were cultured in erythroid differentiation medium containing erythropoietin for 5 d. Cells were subjected to analysis of GFP and RPS19mt-Flag expression using flow cytometry. As shown in Fig 2A and B, in the GFP-positive fraction, RPS19mt-Flag proteins were produced at significantly low levels compared with wild-type levels, except for one mutant, G120R, regardless of the *in vitro* culture conditions.

These results indicate that, like the haematopoietic cell line K562, haematopoietic progenitor cells transfected with a mutated *RPS19* gene can not produce mutant RPS19 protein to the same levels that they can produce wild-type protein.

Down-regulation of RPS19 by siRNA induces cell cycle arrest at G0/G1

Once it was clear that *RPS19* mutations result in a loss of protein production, we thought it suitable to downregulate *RPS19* to study the effects of RPS19-mutated DBA *in vitro*. To analyse the effect of downregulation of RPS19 on cell proliferation, we prepared two different lentivirus vectors expressing different siRNA sequences against RPS19, si-A and si-C. The construction of these siRNAs has been reported previously [Flygare *et al* (2005), see experimental procedure]. K562 cells were transduced with si-A-, si-C- and control sequence (scr)-containing vectors after staining with or without PKH26, which stains the cell membrane. As PKH26 ubiquitously labels the cell membrane, its fluorescence intensity will decrease (in theory by one-half) each time the cell divides. Thus, flow cytometric analysis of the intensity of PKH26 enabled determination whether or not cells have divided since being labelled (Huang *et al*, 1999; Mantel *et al*, 2001). At day-4 postinfection, we confirmed the percentage of infectivity and viability at a multiplicity of infection (MOI) of 10. si-A and si-C repressed the expression of *RPS19*, as shown in Fig 3A. The lentiviral vector containing si-C demonstrated a strong repressive effect on *RPS19* expression. On FACS analysis, the percentage of GFP-positive cells, which indicates transfection of cells with the lentiviral siRNA vectors, was more than 95%, and PI staining indicated that more than 99·5% of the GFP-positive cells were alive in all experiments.

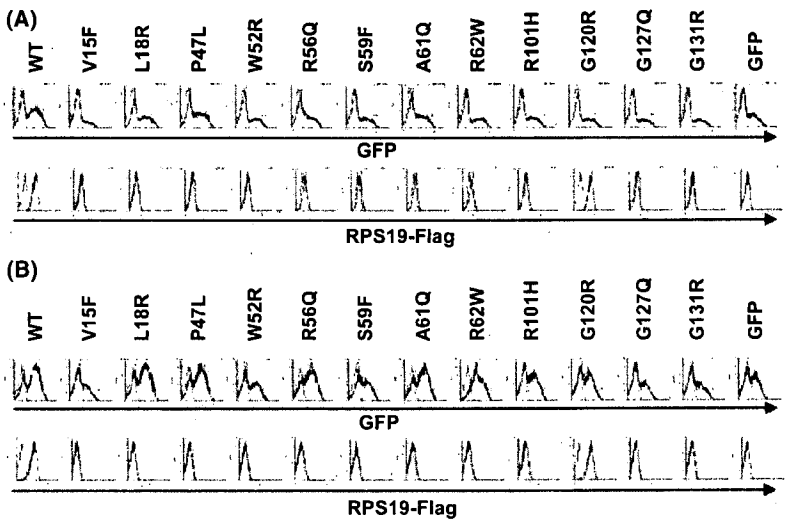

Fig 2. Expression analysis of RPS19 mutants in human bone marrow (BM) cell culture BM $CD34^+$ cells were transduced with retrovirus vector expressing RPS19, RPS19mt or control. About half of the transduced cells were cultured in the presence of SCF, TPO and Flt3-L for 3 d (A). The other half were cultured in the presence of erythropoietin for 5 d. (B) Cells were fixed and stained with Flag M2 antibody followed by staining with APC-conjugated anti-mouse IgG. GFP (upper panel) and APC (lower panel) signals were analysed by flow cytometry, and are indicated as thick lines. The thin lines indicate the negative controls (upper panel: mock cells; lower panel: GFP-transduced cells). Data are from one of three experiments with similar results.

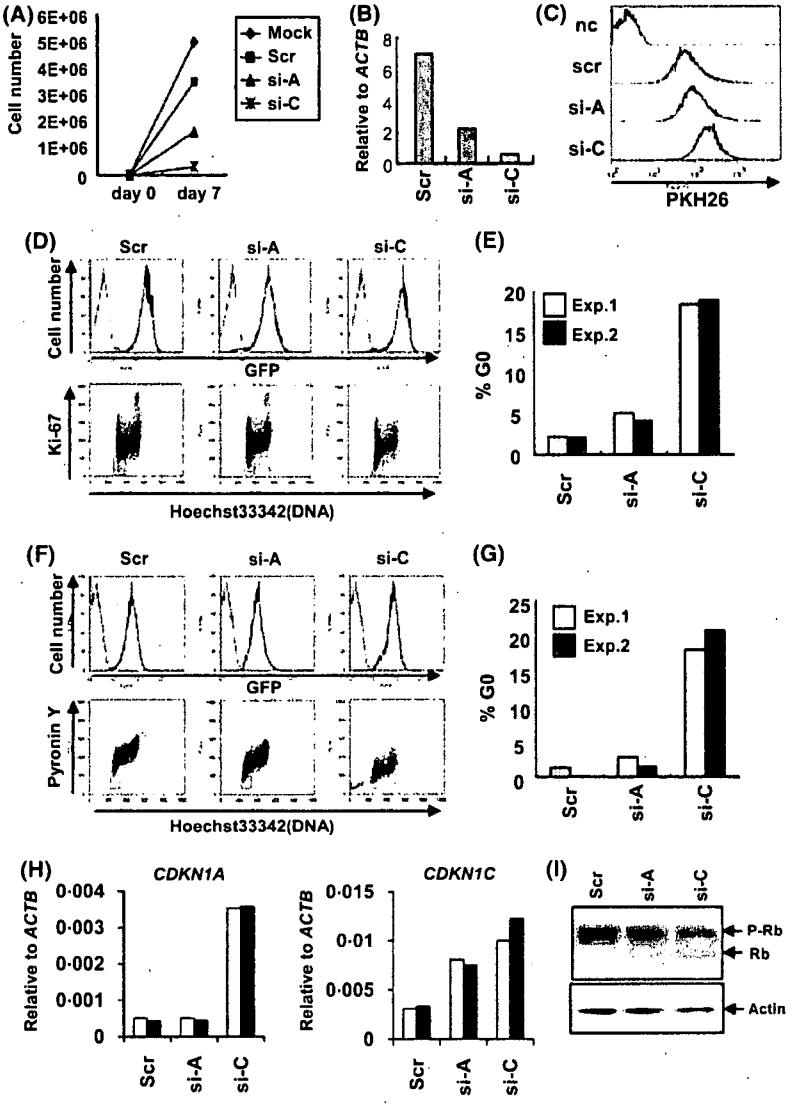

Fig 3. Reduced expression of RPS19 induces G0/G1 arrest in K562 cells. K562 cells were infected with lentivirus vectors expressing siRNAs against *RPS19* (si-A and si-C) or a control siRNA (scr), at a multiplicity of infection (MOI) of 10. Before transduction, cells were stained with or without PKH26. (A) Cell proliferation activity was measured by counting cells at 7 d post-transduction. (B) Cells at 4 d post-transduction were subjected to quantitative RT-PCR analysis of *RPS19* mRNA. Expression levels relative to *ACTB* are indicated. Data are the mean (±SEM) from three separate experiments. (C) The intensity of PKH26 staining in cells at 4 d post-transduction was analysed by flow cytometry. nc indicates negative control. Data are from one of three experiments with similar results. (D) Cells at day 4 post-transduction were subjected to cell cycle analysis. After staining with anti-Ki-67 antigen and Hoechest33342, GFP-positive cells (upper panel) were gated and analysed by flow cytometry. In the lower panel, the horizontal axis indicates DNA content and the longitudinal axis indicates the expression of Ki-67. (E) Percentage of cells in G0 (Ki67- and at stage 2N based on DNA content). Data shows two separate experiments. (F) Fixed cells were stained with Pyronin Y and Hoechst33342, and then GFP-positive cells (upper panel) were gated and analysed by flow cytometry. In the lower panel, the horizontal axis indicates DNA content and the longitudinal axis indicates the signal level of Pyronin Y. (G) Percentage of cells in G0 (Pyronin Y low and at stage 2N based on DNA content). Data show two separate experiments. (H) Cells at 4 d post-transduction were subjected to quantitative RT-PCR analysis of *CDKN1A* and *CDKN1C* mRNA. Expression levels relative to *ACTB* are indicated. Data show two separate experiments. (I) Cells at 4 d post-transduction were analysed for the expression of Rb protein by Western blot analysis. 'P-Rb' indicates the phosphorylated form of Rb protein and 'Rb' indicates the dephosphorylated form of Rb protein. Western blot analysis of β-actin was performed as a control.

As previously reported (Ebert *et al*, 2005; Flygare *et al*, 2005), a decrease in cell proliferation activity was also observed in K562 cells expressing siRNAs against *RPS19* (Fig 3B).

At day-4 post-transduction, the intensity of PKH26 was analysed by flow cytometry. Interestingly, the intensity of PKH26 was high in cells expressing siRNAs against *RPS19*

(Fig 3C). Next, cell cycle profiles were analysed by staining cells with Ki-67 and Hoechst33342. Ki-67 antigen expression is high during G2 and M phases, low at G1, and lost at G0 in the cell cycle (Fig 3D and E). Surprisingly, expression of siRNA against *RPS19* resulted in an increase in the number of cells that were Ki-67 negative and at the 2N stage based on DNA content, indicating arrest of the cell cycle at G0. A similar result was obtained by analysis of the cell cycle based on combined staining with Pyronin Y and Hoechst33342 (Fig 3F and G). Cells expressing siRNAs against *RPS19* were observed to be predominantly at the 2N stage, based on DNA content, and showed a significantly low level of RNA expression, indicating that these cells were in the G0 phase of the cell cycle.

Elevation of *CDKN1A* mRNA level in si-C-transduced cells and elevation of *CDKN1C* mRNA levels in si-A- and si-C-transduced cells were observed when quantitative PCR were performed with cDNA synthesized from siRNA-transduced cells (Fig 3H).

Western blot analysis of retinoblastoma protein (pRb) expression in K562 cells expressing *RPS19* siRNAs was performed at 4 d post-transduction. Interestingly, the dephosphorylated form of pRb accumulated in cells expressing siRNAs against *RPS19* (Fig 3I). These cells were thought not to be able to enter the S phase, in agreement with data from cell cycle analysis based on Ki-67 and Hoechst33342 staining.

These results suggested that downregulation of RPS19 results in low levels of Rb phosphorylation, subsequently inducing G0/G1 arrest in K562 cells.

G0/G1 arrest induced by RPS19 mutations in human haematopoietic progenitor cells causes impaired erythroid lineage commitment

Next, we tried to determine if the same results would be observed in primary human BM $CD34^+$ cells. Bone marrow $CD34^+$ cells were transduced with lentiviral vectors containing scr, si-A and si-C at a MOI of 10, after staining with or without PKH26. At day-4 post-transduction, cells were analysed by flow cytometry. The percentages of $CD34^+$ cells expressing scr, si-A and si-C were 40 ± 17%, 43 ± 15% and 55 ± 15% respectively. The cell cycle profiles were analysed by staining with Ki-67 and Hoechst33342 (Fig 4A). Expression of siRNAs against *RPS19* led to an accumulation of $CD34^+$ cells that were Ki-67 negative and in the 2N stage based on DNA content, indicating that these cells were in G0 arrest. As shown in Fig 4B, the proportion of si-C-transfected cells in G0 was high (8·7 ± 2·2%) compared with scr-transfected cells (3·8 ± 0·6%).

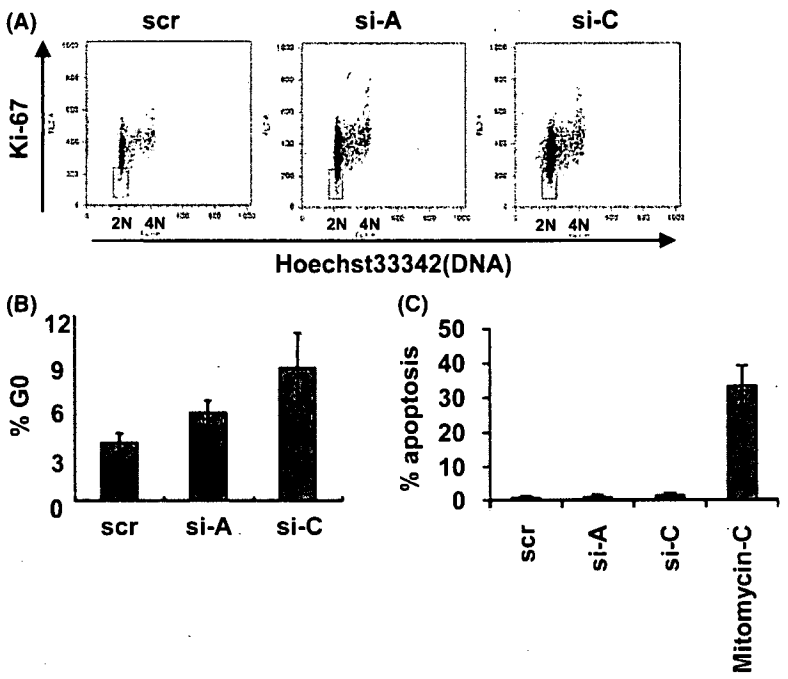

Fig 4. Reduced expression of RPS19 induces G0/G1 arrest in BM progenitor cells (A) BM $CD34^+$ cells were transduced with lentiviral vectors at a MOI of 10. Cells at 4 d post-transduction were subjected to cell cycle analysis. After staining with anti-Ki-67 antigen and Hoechest33342, GFP-positive cells were gated and analysed by flow cytometry. The horizontal axis indicates DNA content and the longitudinal axis indicates the signal level of Ki-67 antigen. (B) Percentage of cells in G0. Data are the mean (±SEM) from three separate experiments. (C) Apoptotic cells were observed by staining with annexin V and PI. After staining GFP positive cells were gated and analysed by flow cytometry. As a positive control of the induction of apoptosis, mitomycin-C was added to medium (10 μg/ml) for 12 h. Data are the mean (±SEM) from three separate experiments.

Around 5·8% of si-A-transfected cells were in G0. The percentage of apoptotic cells was analysed by staining cells with annexin V and PI. The percentages of annexin V-positive and PI-negative cells in the GFP positive fraction were less than 2% in all experiments. Progenitor cell analysis based on CD45RA and CD71 expression showed a specific decrease in the amount of erythroid progenitors (CD71 high$^+$, CD45RA$^-$) among si-C-transfected cells, although the amount of myeloid progenitors (CD71 low$^+$, CD45RA$^+$) was not altered (Fig 5A and B). Quantitative RT-PCR of *RPS19* mRNA was performed against cDNA synthesized from FACS-sorted erythroid and myeloid progenitors that were transduced siRNA. The efficiency of siRNA against *RPS19* mRNA on erythroid progenitors were about 25% (si-A) and 55% (si-C) compared with scr

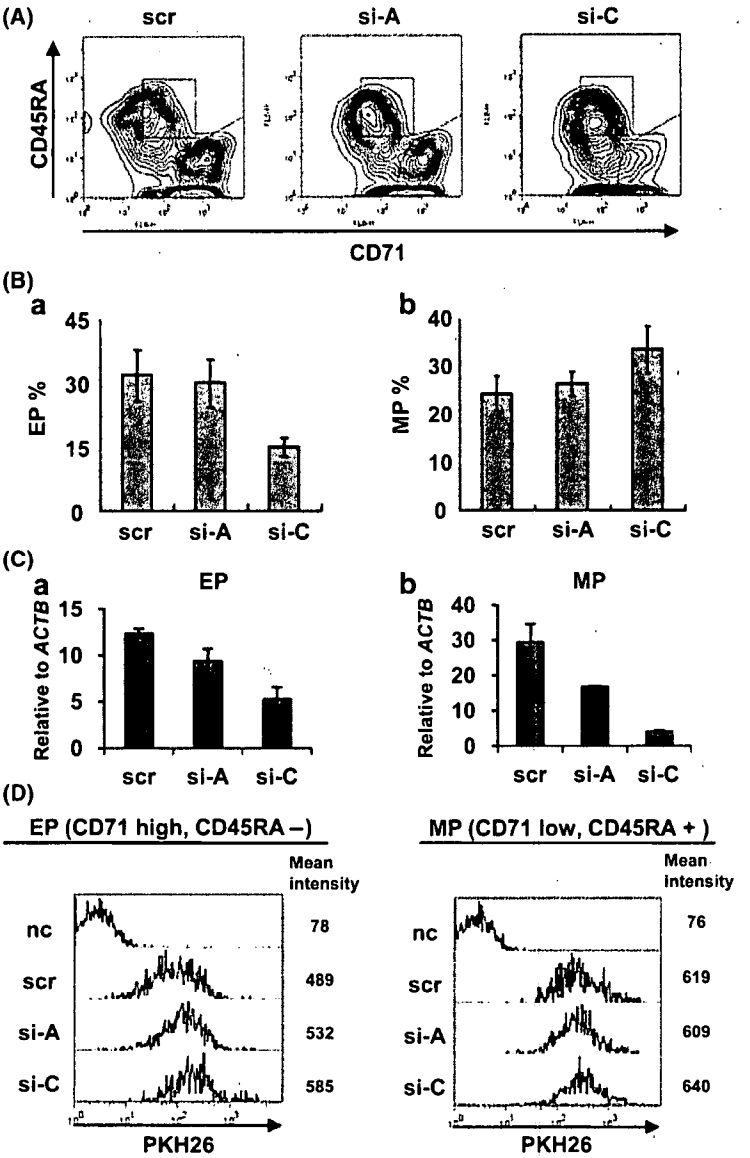

Fig 5. Effect of reduced expression of RPS19 on erythroid progenitors. BM CD34$^+$ cells were transduced with lentiviral vectors at a MOI of 10. Before transduction, cells were stained with PKH26. Cells at 4 d post-transduction were stained with CD71 and CD45RA. Cells that were positive for GFP were gated and analysed based on the intensity of PKH26, CD71 and CD45RA, by flow cytometry. (A) Analysis of the proportion of erythroid progenitors (CD71 high$^+$ and CD45RA$^+$) and myeloid progenitors (CD71 low$^+$, CD45RA$^-$). (B) Percentages of erythroid (B-a) and myeloid (B-b) progenitors. Data are the mean (±SEM) from three separate experiments. (C) At 4 d post-transduction, erythroid (EP) (C-a) and myeloid (MP) (C-b) progenitors were sorted using flow cytometry and were subjected to quantitative RT-PCR analysis of *RPS19* mRNA. Expression levels relative to *ACTB* are indicated. Data are the mean (±SEM) from three separate experiments. (D) The intensity of PHK26 in erythroid (a) and myeloid (b) progenitors. Data are from one of three experiments with similar results.

(Fig 5C-a), which was a mild effect compared to that of K562 and myeloid progenitors [about 45% (si-A) and 85% (si-C)] (Fig 5C-b). Interestingly, the intensity of PKH26 in the erythroid progenitor (CD71 high$^+$, CD45RA$^-$) fraction expressing si-C remained high compared with that in the erythroid progenitor fraction expressing scrambled siRNA (mean intensity: 585 and 489 respectively), whereas the intensity of PKH26 in CD71 low$^+$, CD45RA$^+$ fraction was similar (Fig 5D). The side scatter and forward scatter profiles did not differ between erythroid progenitors and myeloid progenitors, indicating that the cell sizes were similar. The same tendency was observed in three independent experiments. These data indicated that, in primary cells, downregulation of *RPS19* results in G0 arrest and specific regression of erythroid progenitor cell proliferation.

Coincidently, the percentage of erythroid progenitors among BM cells in which *RPS19* was downregulated by siRNA was significantly low compared with that among control siRNA-transfected cells (Fig 5B-a); this tendency was similar to previously reported findings from the analysis of the BMs of DBA patients (Hamaguchi *et al*, 2003).

Discussion

Many questions regarding DBA remain to be answered and this study focused on two of them. First, why do all the various types of mutation in *RPS19* cause a DBA-specific phenotype, congenital anaemia, have in common? Second, why does RPS19 deficiency cause a defect only in the erythroid lineage in DBA haematopoietic cells?

In order to clarify the mechanism of ribosome protein S19 synthesis in haematopoietic progenitor cells, we analysed 12 different mutations identified in individual DBA patients. With the exception of the G120R mutation, RPS19 protein production was not completed in cells expressing *RPS19* containing these mutations. Detailed analysis of RPS19 synthesis using a bi-cistronic vector system demonstrated that transcription must occur, because the expression of GFP from mutant RPS19-containing vectors was equal to that of controls. Moreover mutant RPS19 proteins were analysed in the presence of the proteosome inhibitor MG132. As MG132 rescued the repression of mutant RPS19 protein, the extinction of mutant RPS19 was caused by protein degradation in the proteosome. These results suggest that the expression of RPS19 protein is strictly regulated after translation. Only the G120R mutant is sufficiently expressed in both K562 and CD34$^+$ haematopoietic progenitor cells. We do not have data to explain how this mutant is associated with the DBA phenotype; however, this mutant maybe a useful tool with which to obtain RPS19 interacting molecules involved in anaemia, by comparing the interactomes of wild-type RPS19 and the G120R mutant.

Concerning the various other types of *RPS19* mutations, such as deletions, non-sense mutations and frame shifts, the expression level of RPS19 proteins was reported to be low in patients with DBA (Hamaguchi *et al*, 2002; Chatr-Aryamontri *et al*, 2004; Gazda *et al*, 2004). We previously shown that cells obtained from four DBA patient cells with missense mutations, translocation, and entire loss of an *RPS19* allele, partially recovered the ability for erythroid colony formation following the forced expression of normal RPS19 (Hamaguchi *et al*, 2002). These findings suggested that protein production from the mutant *RPS19* genes of DBA patients may be repressed similar to that of the single-point mutated *RPS19* constructs in this study.

Recently the function of RPS19 in ribosome biogenesis has been reported. Depletion of RPS19 alters pre-18S rRNA processing and blocks the maturation of the 40S ribosome in yeast. Moreover, downregulation of *RPS19* by siRNA induces defects in pre-18S rRNA in cultured human cells (Leger-Silvestre *et al*, 2005; Choesmel *et al*, 2007; Flygare *et al*, 2007). These findings suggest that decreased expression of mutant RPS19 contributes to abnormal ribosomal synthesis at the first step of DBA pathogenesis. However, the association between the alteration of pre-18S rRNA processing and the cell proliferation defect remains to be clarified.

In order to elucidate the mechanism underlying the proliferation defect in the BM cells of DBA patients, we analysed the biological effects of RPS19 in K562 cells and CD34$^+$ haematopoietic cells. As shown in Figs 3 and 4, decreased levels of RPS19 caused G0/G1 arrest in K562 and CD34$^+$ cells. Inadequate cell cycle regulation in haematopoietic cells is likely to be a critical step in the development of severe anaemia. Fanconi anaemia (FA) is a genetic disease of cancer susceptibility marked by congenital defects, BM failure and myeloid leukaemia (Mi & Kupfer, 2005). Cells derived from patients with this disease exhibit G2-phase cell cycle delay, and secondary defects of the S or G2 checkpoint.

Some inherited BM failure syndromes, including dyskeratosis congenita (DC), cartilage-hair hypoplasia (CHH) and Shwachman–Diamond syndrome (SDS), are characterized by BM failure and the variable presence of congenital anomalies and cancer predisposition. Intriguingly, the genes mutated in these disorders encode factors involved in ribosome synthesis, suggesting a link between this fundamental cellular process and marrow failure (Liu & Ellis, 2006). Recently, an extraribosomal function of RPL26 was revealed: this molecule also acts as a regulator of the cell cycle, and induces G1 arrest in *Drosophila* (Takagi *et al*, 2005). In human haematopoietic cells, a similar molecular mechanism involving ribosomal function may contribute to cell cycle arrest.

We also revealed that Rb-phospholylation was altered in RPS19-deficient cells. The sequential phosphorylation and subsequent inactivation of Rb is an important part of cell cycle regulation and haematopietic differentiation (Walkley *et al*, 2007). Rb is phosphorylated by cyclin-cyclin-dependent kinase (Cdk) complexes. Several negative regulators of Cdk activity have been studied in the context of HSC biology. Loss of the Cdk2 inhibitors p21Cip1 (Cheng *et al*, 2000a) and p27Kip (Cheng *et al*, 2000b) revealed a divergent role in HSC

regulation, with a loss of p21Cip1 resulting in a subtle increase in sensitivity to stress-induced exhaustion, apparent *in vivo* after quaternary transplant. Loss of p27Kip1 resulted in a twofold increase in the number of long-term repopulating HSCs in addition to an enlarged progenitor compartment. Collectively, these studies suggest that negative cell-cycle regulators that impact directly on Rb-family protein function may influence HSC fate.

In this study, we tried to compare the effects of different types of RPS19 deficiency. In K562 cells expressing si-A or si-C siRNAs against *RPS19*, the expression of *RPS19* mRNA was repressed by 70% and 90% respectively. Repression of RPS19 protein production in si-C-transduced cells led to a decrease in the level of phosphorylated Rb, and this decrease was much less than that observed in si-A-transduced cells (Fig 3I). This means that, in proportion to the suppressive expression of RPS19, cell cycle arrest was severe. These findings suggest that inhibition of Rb phosphorylation may be a key step in DBA models, leading to increased cell cycle arrest at the G0/G1 stage.

The next question is why the proliferation defects are specific for the erythroid lineage. As shown in Fig 5, the distribution analysis of haematopoietic progenitors with cell surface antigen demonstrated that si-C transduction caused an erythroid progenitor-specific defect that was coincident with that observed in the cells of DBA patients (Hamaguchi *et al*, 2002); however, si-A did not cause this abnormal distribution as well as a scrambled control siRNA. This might be due to the insufficiency of siRNA downregulation because quantitative RT-PCR data indicated that si-A did not downregulate *RPS19* mRNA in primary BM erythroid progenitor cells as efficiently as in K562 cells (Figs 3B and 5C-a, -b). PKH26 staining of erythroid cells demonstrated that the PKH26 intensity of si-C-transduced erythroid progenitors was relatively high compared with that of scr-transduced cells. Interestingly, si-A-transduced cells did not demonstrate severe defects of the erythroid lineage. Furthermore, among myeloid progenitors, we could not find these differences in cells expressing scr, si-A or si-C. These findings suggest that the severe defect in RPS19 production negatively regulates erythroid differentiation. Erythroid-specific retardation may be affected by the difference in the rate of cell cycle in between progenitors, because the intensity of PKH26 in the erythroid progenitor fraction was low compared with that in the myeloid progenitor fraction among control siRNA-transduced cells.

It was reported that elevated apoptotic activity was observed in cells from DBA patients (Perdahl *et al*, 1994). But apoptotic cells were not predominantly observed both in RPS19 downregulated K562 and BM $CD34^+$ cells throughout our experiments. Our data demonstrated that specific decrease of erythroid progenitors can be induced by the cell cycle arrest in association with the downregulation of RPS19, without apoptotic induction. In this setting, downregulation of RPS19 was observed both in the erythroid and myeloid progenitors. However, retardation of the cell proliferation was observed only in the erythroid progenitors, which may possibly be a result of the difference in sensitivity to the induction of cell cycle arrest.

Although it is still unclear whether the cell proliferation blockage through G0/G1 arrest induced *in vitro* by siRNA is true of the BM cells of DBA patients, haematopoietic progenitors in an abnormal cell cycle state mimic the DBA phenotype. Our findings will improve our understanding of the relationship between haematopoietic disease and cell-cycle abnormalities. Further analysis regarding ribosomal stress and human disease is needed.

Acknowledgements

The authors thank Ms Momoka Tsuruhara and Ms Keiko Furuhata for expert assistance. This work was supported by Grants-in-Aid from the Ministry of Education, Science, Technology, Sports, and Culture, Japan.

References

Chatr-Aryamontri, A., Angelini, M., Garelli, E., Tchernia, G., Ramenghi, U., Dianzani, I. & Loreni, F. (2004) Nonsense-mediated and nonstop decay of ribosomal protein S19 mRNA in Diamond-Blackfan anemia. *Human Mutation*, **24**, 526–533.

Cheng, T., Rodrigues, N., Dombkowski, D., Stier, S. & Scadden, D.T. (2000a) Stem cell repopulation efficiency but not pool size is governed by p27(kip1). *Nature Medicine*, **6**, 1235–1240.

Cheng, T., Rodrigues, N., Shen, H., Yang, Y., Dombkowski, D., Sykes, M. & Scadden, D.T. (2000b) Hematopoietic stem cell quiescence maintained by p21cip1/waf1. *Science*, **287**, 1804–1808.

Choesmel, V., Bacqueville, D., Rouquette, J., Noaillac-Depeyre, J., Fribourg, S., Cretien, A., Leblanc, T., Tchernia, G., Da Costa, L. & Gleizes, P.E. (2007) Impaired ribosome biogenesis in Diamond-Blackfan anemia. *Blood*, **109**, 1275–1283.

Cmejla, R., Blafkova, J., Stopka, T., Zavadil, J., Pospisilova, D., Mihal, V., Petrtylova, K. & Jelinek, J. (2000) Ribosomal protein S19 gene mutations in patients with diamond-blackfan anemia and identification of ribosomal protein S19 pseudogenes. *Blood Cells, Molecules, and Diseases*, **26**, 124–132.

Da Costa, L., Tchernia, G., Gascard, P., Lo, A., Meerpohl, J., Niemeyer, C., Chasis, J.A., Fixler, J. & Mohandas, N. (2003) Nucleolar localization of RPS19 protein in normal cells and mislocalization due to mutations in the nucleolar localization signals in 2 Diamond-Blackfan anemia patients: potential insights into pathophysiology. *Blood*, **101**, 5039–5045.

Diamond, L.K., Wang, W.C. & Alter, B.P. (1976) Congenital hypoplastic anemia. *Advances in Pediatrics*, **22**, 349–378.

Draptchinskaia, N., Gustavsson, P., Andersson, B., Pettersson, M., Willig, T.N., Dianzani, I., Ball, S., Tchernia, G., Klar, J., Matsson, H., Tentler, D., Mohandas, N., Carlsson, B. & Dahl, N. (1999) The gene encoding ribosomal protein S19 is mutated in Diamond-Blackfan anaemia. *Nature Genetics*, **21**, 169–175.

Ebert, B.L., Lee, M.M., Pretz, J.L., Subramanian, A., Mak, R., Golub, T.R. & Sieff, C.A. (2005) An RNA interference model of RPS19 deficiency in Diamond-Blackfan anemia recapitulates defective hematopoiesis and rescue by dexamethasone: identification of dexamethasone-responsive genes by microarray. *Blood*, **105**, 4620–4626.

Flygare, J., Kiefer, T., Miyake, K., Utsugisawa, T., Hamaguchi, I., Da Costa, L., Richter, J., Davey, E.J., Matsson, H., Dahl, N., Wiznerowicz, M., Trono, D. & Karlsson, S. (2005) Deficiency of ribosomal protein S19 in CD34+ cells generated by siRNA blocks erythroid development and mimics defects seen in Diamond-Blackfan anemia. *Blood*, **105**, 4627–4634.

Flygare, J., Aspesi, A., Bailey, J.C., Miyake, K., Caffrey, J.M., Karlsson, S. & Ellis, S.R. (2007) Human RPS19, the gene mutated in Diamond-Blackfan anemia, encodes a ribosomal protein required for the maturation of 40S ribosomal subunits. *Blood*, **109**, 980–986.

Gazda, H.T., Zhong, R., Long, L., Niewiadomska, E., Lipton, J.M., Ploszynska, A., Zaucha, J.M., Vlachos, A., Atsidaftos, E., Viskochil, D.H., Niemeyer, C.M., Meerpohl, J.J., Rokicka-Milewska, R., Pospisilova, D., Wiktor-Jedrzejczak, W., Nathan, D.G., Beggs, A.H. & Sieff, C.A. (2004) RNA and protein evidence for haplo-insufficiency in Diamond-Blackfan anaemia patients with RPS19 mutations. *British Journal of Haematology*, **127**, 105–113.

Gazda, H.T., Grabowska, A., Merida-Long, L.B., Latawiec, E., Schneider, H.E., Lipton, J.M., Vlachos, A., Atsidaftos, E., Ball, S.E., Orfali, K.A., Niewiadomska, E., Da Costa, L., Tchernia, G., Niemeyer, C., Meerpohl, J.J., Stahl, J., Schratt, G., Glader, B., Backer, K., Wong, C., Nathan, D.G., Beggs, A.H. & Sieff, C.A. (2006) Ribosomal protein S24 gene is mutated in Diamond-Blackfan anemia. *American Journal of Human Genetics*, **79**, 1110–1118.

Hamaguchi, I., Ooka, A., Brun, A., Richter, J., Dahl, N. & Karlsson, S. (2002) Gene transfer improves erythroid development in ribosomal protein S19-deficient Diamond-Blackfan anemia. *Blood*, **100**, 2724–2731.

Hamaguchi, I., Flygare, J., Nishiura, H., Brun, A.C., Ooka, A., Kiefer, T., Ma, Z., Dahl, N., Richter, J. & Karlsson, S. (2003) Proliferation deficiency of multipotent hematopoietic progenitors in ribosomal protein S19 (RPS19)-deficient diamond-Blackfan anemia improves following RPS19 gene transfer. *Molecular Therapy*, **7**, 613–622.

Huang, S., Law, P., Francis, K., Palsson, B.O. & Ho, A.D. (1999) Symmetry of initial cell divisions among primitive hematopoietic progenitors is independent of ontogenic age and regulatory molecules. *Blood*, **94**, 2595–2604.

Leger-Silvestre, I., Caffrey, J.M., Dawaliby, R., Alvarez-Arias, D.A., Gas, N., Bertolone, S.J., Gleizes, P.E. & Ellis, S.R. (2005) Specific role for yeast homologs of the Diamond Blackfan anemia-associated Rps19 protein in ribosome synthesis. *Journal of Biological Chemistry*, **280**, 38177–38185.

Lipton, J.M. (2006) Diamond blackfan anemia: new paradigms for a "not so pure" inherited red cell aplasia. *Seminars in Hematology*, **43**, 167–177.

Liu, J.M. & Ellis, S.R. (2006) Ribosomes and marrow failure: coincidental association or molecular paradigm? *Blood*, **107**, 4583–4588.

Mantel, C., Hendrie, P. & Broxmeyer, H.E. (2001) Steel factor regulates cell cycle asymmetry. *Stem Cells*, **19**, 483–491.

Matsson, H., Davey, E.J., Frojmark, A.S., Miyake, K., Utsugisawa, T., Flygare, J., Zahou, E., Byman, I., Landin, B., Ronquist, G., Karlsson, S. & Dahl, N. (2006) Erythropoiesis in the Rps19 disrupted mouse: analysis of erythropoietin response and biochemical markers for Diamond-Blackfan anemia. *Blood Cells, Molecules, and Diseases*, **36**, 259–264.

Mi, J. & Kupfer, G.M. (2005) The Fanconi anemia core complex associates with chromatin during S phase. *Blood*, **105**, 759–766.

Miyake, K., Flygare, J., Kiefer, T., Utsugisawa, T., Richter, J., Ma, Z., Wiznerowicz, M., Trono, D. & Karlsson, S. (2005) Development of cellular models for ribosomal protein S19 (RPS19)-deficient diamond-blackfan anemia using inducible expression of siRNA against RPS19. *Molecular Therapy*, **11**, 627–637.

Orfali, K.A., Ohene-Abuakwa, Y. & Ball, S.E. (2004) Diamond Blackfan anaemia in the UK: clinical and genetic heterogeneity. *British Journal of Haematology*, **125**, 243–252.

Perdahl, E.B., Naprstek, B.L., Wallace, W.C. & Lipton, J.M. (1994) Erythroid failure in Diamond-Blackfan anemia is characterized by apoptosis. *Blood*, **83**, 645–650.

Proust, A., Da Costa, L., Rince, P., Landois, A., Tamary, H., Zaizov, R., Tchernia, G. & Delaunay, J. (2003) Ten novel Diamond-Blackfan anemia mutations and three polymorphisms within the rps19 gene. *Hematol J*, **4**, 132–136.

Ramenghi, U., Campagnoli, M.F., Garelli, E., Carando, A., Brusco, A., Bagnara, G.P., Strippoli, P., Izzi, G.C., Brandalise, S., Riccardi, R. & Dianzani, I. (2000) Diamond-Blackfan anemia: report of seven further mutations in the RPS19 gene and evidence of mutation heterogeneity in the Italian population. *Blood Cells, Molecules, and Diseases*, **26**, 417–422.

Takagi, M., Absalon, M.J., McLure, K.G. & Kastan, M.B. (2005) Regulation of p53 translation and induction after DNA damage by ribosomal protein L26 and nucleolin. *Cell*, **123**, 49–63.

Vladimirov, S.N., Ivanov, A.V., Karpova, G.G., Musolyamov, A.K., Egorov, T.A., Thiede, B., Wittmann-Liebold, B. & Otto, A. (1996) Characterization of the human small-ribosomal-subunit proteins by N-terminal and internal sequencing, and mass spectrometry. *European Journal of Biochemistry*, **239**, 144–149.

Walkley, C.R., Shea, J.M., Sims, N.A., Purton, L.E. & Orkin, S.H. (2007) Rb regulates interactions between hematopoietic stem cells and their bone marrow microenvironment. *Cell*, **129**, 1081–1095.

Willig, T.N., Niemeyer, C.M., Leblanc, T., Tiemann, C., Robert, A., Budde, J., Lambiliotte, A., Kohne, E., Souillet, G., Eber, S., Stephan, J.L., Girot, R., Bordigoni, P., Cornu, G., Blanche, S., Guillard, J.M., Mohandas, N. & Tchernia, G. (1999a) Identification of new prognosis factors from the clinical and epidemiologic analysis of a registry of 229 Diamond-Blackfan anemia patients. DBA group of Societe d'Hematologie et d'Immunologie Pediatrique (SHIP), Gesellshaft fur Padiatrische Onkologie und Hamatologie (GPOH), and the European Society for Pediatric Hematology and Immunology (ESPHI). *Pediatric Research*, **46**, 553–561.

Willig, T.N., Draptchinskaia, N., Dianzani, I., Ball, S., Niemeyer, C., Ramenghi, U., Orfali, K., Gustavsson, P., Garelli, E., Brusco, A., Tiemann, C., Perignon, J.L., Bouchier, C., Cicchiello, L., Dahl, N., Mohandas, N. & Tchernia, G. (1999b) Mutations in ribosomal protein S19 gene and diamond blackfan anemia: wide variations in phenotypic expression. *Blood*, **94**, 4294–4306.

Willig, T.N., Gazda, H. & Sieff, C.A. (2000) Diamond-Blackfan anemia. *Current Opinion in Hematology*, **7**, 85–94.

Wiznerowicz, M. & Trono, D. (2003) Conditional suppression of cellular genes: lentivirus vector-mediated drug-inducible RNA interference. *Journal of Virology*, **77**, 8957–8961.

Molecular Allelokaryotyping of Early-stage, Untreated Chronic Lymphocytic Leukemia

Sören Lehmann, MD[1,2]
Seishi Ogawa, MD[3]
Sophie D. Raynaud, MD[4]
Masashi Sanada, MD[3]
Yasuhito Nannya, MD[3]
Michel Ticchioni, MD[5]
Christian Bastard, MD[6]
Norihiko Kawamata, MD[1]
H. Phillip Koeffler, MD[1]

[1] Department of Hematology/Oncology, Cedars-Sinai Medical Center, University of California at Los Angeles School of Medicine, Los Angeles, California.

[2] Department of Hematology, Karolinska University Hospital, Huddinge, Sweden.

[3] Regeneration Medicine for Hematopoiesis, University of Tokyo, Tokyo, Japan.

[4] Genetics Laboratory, Archet Hospital, Nice, France.

[5] Immunology Laboratory, Archet Hospital, Nice, France.

[6] Genetic Oncology Laboratory, University of Rouen, Rouen, France.

The first 3 authors contributed equally to this work.

The last 2 authors contributed equally to this work.

Address for reprints: Norihiko Kawamata, MD, Department of Hematology/Oncology, Cedars-Sinai Medical Center/UCLA School of Medicine, 8700 Beverly Boulevard, Los Angeles, CA 90048; Fax: (310) 423-0443; E-mail: kawamatan@cshs.org

Received June 7, 2007; revision received September 10, 2007; accepted September 18, 2007.

BACKGROUND. To the authors' knowledge, genetic abnormalities in early-stage chronic lymphocytic leukemia (CLL) have not been examined fully. Single nucleotide polymorphism (SNP) genomic array (SNP-chip) is a new tool that can detect copy number changes and uniparental disomy (UPD) over the entire genome with very high resolution.

METHODS. The authors performed SNP-chip analysis on 56 samples from patients with early-stage, untreated CLL. To validate the SNP-chip data, fluorescence in situ hybridization (FISH) analysis was performed at selected sites. Expression levels of ZAP-70 and the mutational status of immunoglobulin heavy-chain gene also were examined.

RESULTS. SNP-chip analysis easily detected nearly all changes that were identified by FISH, including trisomy 12, deletion of *TP53* (17p13), deletion of *ATM* (11q22), and deletion of 13q14. Only 10 of 56 CLL samples (18%) had no genomic abnormalities. Excluding the 4 common abnormalities mentioned above, 25 CLL samples (45%) had a total of 45 copy number changes detected by SNP-chip analysis. Four samples had 6q deletion at 6q21 that involved the *AIM1* gene. UPD was detected in 4 samples; 2 samples involved whole chromosome 13 resulting in homozygous deletion of micro-RNA-15a (miR-15a)/miR-16-1. CLL samples with deletion of 13q14 and trisomy 12 were mutually exclusive.

CONCLUSIONS. Genetic abnormalities, including whole chromosome 13 UPD, are very common events in early-stage CLL. SNP-chip analysis can detect small genetic abnormalities in CLL and may be able to support or even supplant FISH and cytogenetics. ***Cancer* 2008;112:1296–305.** © *2008 American Cancer Society.*

KEYWORDS: uniparental disomy, micro-RNA, *ATM*, *TP53*, cyclin D2.

Chronic lymphocytic leukemia (CLL) constitutes the most common type of leukemia in the western world.[1] Its clinical course spans from asymptomatic disease to a rapidly progressing course necessitating urgent and intensive treatment.[2] Several prognostic factors have been identified that predict the time to onset of therapy and the survival of patients, including clinical stage as defined by Rai and Binet, lymphocyte doubling time, β2 microglobulin, and expression of CD38 and ZAP-70.[3–5] However, a more robust manner to subclassify CLL is by identifying the genomic changes in the malignant clone. The relative heterogeneity of the disease is reflected by the occurrence of different genetic abnormalities in distinct subclasses of patients. In addition, a strong correlation exists between specific genetic aberrations and the clinical course of the disease.[3–5] CLL can be divided into 2 categories based on the mutational status of the variable region of the immunoglobulin heavy-chain (IgVH). Somatic hypermutation of the *IgVH* gene is observed in >50% of patients, and its presence is associated with a more benign clinical

DOI 10.1002/cncr.23270
Published online 1 February 2008 in Wiley InterScience (www.interscience.wiley.com).

course.[3–5] By using a sensitive tool such as fluorescence in situ hybridization (FISH), genetic abnormalities can be identified in 80% of patients with CLL.[6] Common genetic changes include deletions of the short arm of chromosome 17 and the long arm of chromosome 11 or 13 as well as trisomy of chromosome 12.[6] Deletion of 13q14 is the most common abnormality in CLL[3–5] and, along with hypermutation of *IgVH*, is associated with a good prognosis.[3–5]

A crucial question is how these genetic events participate in the pathogenesis of CLL. Although major uncertainties exist regarding the causative genes, the common deleted regions at 11q and 17p harbor the *ATM* and *TP53* genes, respectively; and these genes also can be mutated in CLL.[3–5] The 13q14 deletion appears more complex. Despite thorough searches by several groups, no mutated or causative gene has been identified within the common deleted region (CDR).[7,8] However, Calin et al recently demonstrated decreased expression and mutations in 2 mirco-RNAs located between exons 4 and 5 of the *DLEU2* gene, in the CDR at 13q14.[9,10] Nevertheless, the role of these micro-RNAs for the pathogenesis of CLL remains unclear. Beside these common abnormalities, genetic alterations in early-stage CLL have not been fully examined.

Recently, high-density, single nucleotide polymorphism (SNP) genomic arrays (SNP-chips) have become available as a tool to screen for new genetic aberrations in malignant cells.[11,12] SNP-chip analysis allows the detection of copy number changes and allelic loss without copy number change, so-called uniparental disomy (UPD), with a resolution that was not obtained with previous methods.[11,12] We named this novel analysis *molecular allelokaryotyping*, because this technique allows us to examine genetic status at the molecular level and to evaluate allele-specific gene dosage in cancer cells.[13] In the current study, we performed molecular allelokaryotyping on 56 samples of early-stage (Binet stage A) CLL using the 50-k Xba GeneChip from Affymetrix (50,000 SNP probes).

MATERIALS AND METHODS

Patients and Samples

We studied 56 untreated patients with B-cell CLL at Binet stage A who were diagnosed using standard immunophenotypic criteria.[4] All patients had typical morphologic features of CLL and had immunophenotypic scores of 4 or 5 according to the scoring system proposed by Matutes et al.[14] The percentage of CLL cells in peripheral blood ranged between 38% and 98% at diagnosis (mean, 77%). Lymphocyte doubling times in all patients before treatment were >12 months. Thirty patients were men, and 26 were women; and the median age at diagnosis was 69 years (range, 51-86 years). Peripheral blood mononuclear cells were purified by Ficoll gradient and were used as sample material. Chromosomal analysis of CLL cells was performed according to the standard technique. Results of chromosomal analysis were obtained from 49 patients. This protocol was approved by the local ethical committee Comites de Protection des Personnes dans la Recherche Biomedicale (CPPRB) of the Central University Hospital in Nice.

SNP-Chip Analysis

SNP-chips (GeneChip Human mapping 50-k array *Xba*I 240; Affymetrix Japan, Tokyo, Japan) were used for this study. Fragmentation and labeling of DNAs were performed by using a GeneChip resequencing kit (Affymetrix Japan) according to the manufacturer's protocols. Hybridization, washing and signal detection were performed on a GeneChip Fluidics Station 400 and a GeneChip scanner 3000 according to the manufacturer's protocols (Affymetrix, Japan). The data were analyzed by a newly developed program, the copy number analysis for Affymetrix GeneChips (CNAG) program, as described previously.[12,13] By using this program, we were able to obtained allele-specific gene dosage levels of the samples (without matched control samples) by comparing the data with pooled data of normal DNA from volunteers.[13] The results were observed and all genomic abnormalities were examined manually.

Allelelic Dosage Analysis by Real-time Polymerase Chain Reaction

Allelic dosage was measured by real-time polymerase chain reaction (PCR) using genomic DNA extracted from the patients or healthy volunteers. The primers used for allelic dosage analysis are listed in the Supplement Table (available at URL: http://research.csmc.edu/paper/kawamata/CLL.pdf. Accessed on December 25, 2007).

FISH

Peripheral blood smear samples from patients were used for interphase FISH analysis. The FISH studies were performed using the LSI-p53 (17p13)/LSI-*ATM* (11q22) and LSI-13S319 (13q14). 13q34/CEP-12 (chromosome 12) Multicolor Probe sets purchased from Abbott Molecular Inc. (Rungis Cedex, France). Three hundred nuclei were analyzed for each probe set. The cutoff for positive values was 20% for deletion of *ATM* and *TP53*, 9% for 13q14 deletions, and 15% for trisomy 12.

Mutation Status Analysis of the *IgVH* Gene

Genomic DNA was isolated by using standard proteinase K/phenol/chloroform extraction methods.[15] Amplification of the VDJ rearrangements was performed by PCR using framework region 1 and JH family-specific consensus primers, as described previously.[16] The VDJ nucleotide sequences were determined directly and were compared with reported human genome sequences.[16] When a sample demonstrated that <2% of base pairs differed from the reported consensus sequence, it was considered ummutated.[16]

Determination of Genomic Sequences of the *TP53* and *AIM1* Genes

To determine nucleotide sequences, genomic DNA from CLL cells was used as a template. Genomic DNA encoding exons 4, 5, 6, 7, and 8 of the *TP53* gene and all 20 exons of the *AIM1* gene were amplified by PCR with the specific primers. The PCR products were separated in 2.5% agarose gel and purified. Sequences were determined directly by using the purified PCR products. The PCR product of the *TP53* gene was cloned further into pCR 2.1 TOPO vector (Invitrogen, Carlsbad, Calif), and the product was sequenced.

Analysis of Methylation Status of the AIM1 Gene

Genomic DNA was modified by sodium bisulfate using the EZ DNA Methylation Kit (Zymo Research, Orange, Calif). The CpG island of the *AIM1* gene (from −26 to +898; the transcription initiation site was considered as +1) in CLL cells was amplified from the modified genomic DNA as a template by using bisulfate-modified, DNA-specific primers (sense primer: 5′-TTG GAG GTA GAG GGA GAG TTT TT-3′; antisense primer: 5′-CAC CCT CTT AAA TAA AAA CTC C-3′). The PCR products were digested with *BstUI* restriction endonucleases to analyze the methylation status of the CpG island, as reported previously.[17]

ZAP Expression

ZAP-70 expression was determined by flow cytometry on lymphoid cells as described previously with minor modifications.[16] Briefly, cells were incubated with phycoerythrin (PE)-CD56, PE-CD3, peridin-chlorophyll protein-indodicarbocyanine 5-CD19 (Becton-Dickinson, San Jose, Calif), and APC-CD5 antibodies (Pharmingen, San Jose, Calif), then fixed and permeabilized by using the Fix & Perm kit according to manufacturer's instructions (Caltag Laboratories, Burlingame, Calif). Cells were incubated with either an anti-ZAP-70 (Upstate, Charlottesville, Va) or an isotype control antibody followed by fluorescein isothiocyanate-antimouse immunoglobulin antibody (SouthernBiotech, Birmingham, Ala). Cells were washed extensively between each step. The percentage of CLL cells that expressed ZAP-70 was calculated by using the gating strategy as described previously.[16] A CLL sample was considered ZAP-70 positive when >20% the CD19-positive/CD5-positive cells expressed ZAP-70.

Correlation Analysis of Genetic Abnormalities and Clinical Status

The clinical status was available for 51 of 56 patients. Correlation of each genetic abnormality and prognosis were examined by chi-square test.

RESULTS

Validation of SNP-Chip Analysis

Initially, we investigated the specificity and sensitivity of SNP-chip analysis to detect known genomic abnormalities as defined by FISH. These studies validated the efficacy of SNP-chip analysis. Five of our 56 CLL samples (9%) had loss of 1 *ATM* (11q22) allele detected by FISH. These samples had 27%, 58%, 58%, 59%, and 59% of cells with heterozygous loss of *ATM* detected by FISH. SNP-chip analysis detected all 5 of these samples with 11q deletion (Figs. 1, 2). SNP-chip also identified 1 sample that had deletion of the 11q22 region that was not detected by FISH (Fig. 2, Patient 44). FISH analysis in this sample indicated that 14% of cells had 11q22 deletion, and the sample was diagnosed as negative for this deletion. However, SNP-chip analysis clearly demonstrated a deletion of 11q14.2 through q24.2 (Fig. 2). Because data on allele-specific gene dosage indicate levels of paternal and maternal alleles, difference in gene dosage between 2 parental alleles can be observed clearly. Hemizygous deletion of 11q14.2 through q24.2 in this specimen is observed clearly by allele-specific gene dosage analysis (Fig. 2).

Three samples (5%) had loss of 1 allele of *TP53* (17p13) in 30%, 39%, and 55% of cells, as detected by FISH. Each of these deletions also was identified by SNP-chip analysis (Fig. 1). Four of our patients (7%) had trisomy 12 in 21%, 25%, 29%, and 54% of cells detected by FISH. SNP-chip analysis identified gain of whole chromosome 12 in all of these patients (Fig. 1).

Deletion of 13q14, which contains micro-RNA-15a (miR-15a)/miR-16-1, is the most common genetic abnormality in CLL.[9] Of the 56 samples of CLL, 33 samples (59%) had a heterozygous and/or homozygous loss of the critical region on 13q14 identified by FISH (Table 1). SNP-chip analysis per-

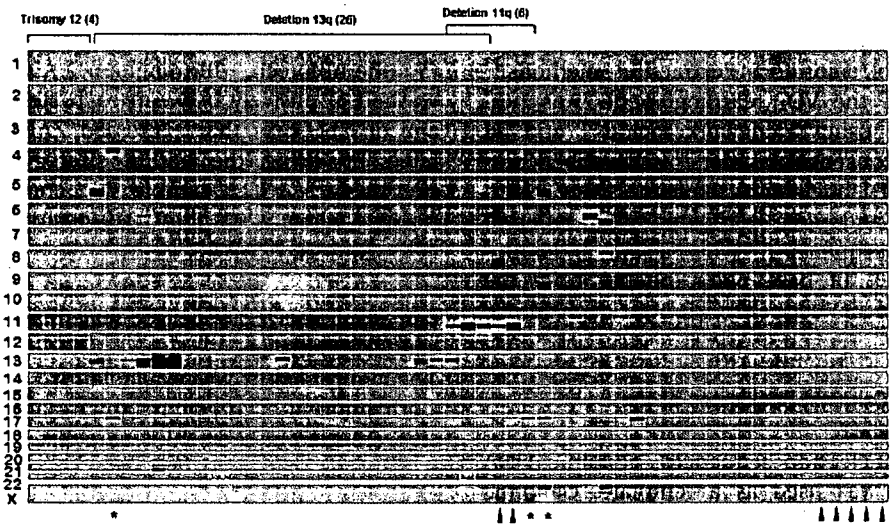

FIGURE 1. Genomic alterations detected by single nucleotide polymorphism (SNP)-chip analysis. Displayed are deletions (blue), amplifications (pink), and uniparental disomy (red) that were identified by SNP-chip analysis. Vertical axis shows chromosomes 1 through X; horizontal axis shows data from 56 patients with chronic lymphocytic leukemia. Upper and lower boxes for each chromosome represent the short and long arms, respectively, of each chromosome. Samples with deletion of *TP53* (17p13) are indicted by asterisks. Samples with 13q14 deletion, which was detected only by fluorescence in situ hybridization analysis, are indicated by triangles. Numbers in parenthesis indicate the number of patients who had each common genetic abnormality identified by SNP-chip analysis.

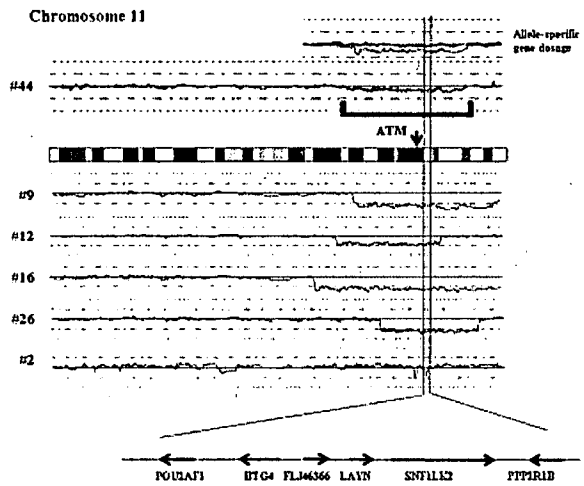

FIGURE 2. Common deleted region of 11q. Single nucleotide polymorphism-chip data from 6 samples of chronic lymphocytic leukemia with deletion of 11q are shown. Each blue line indicates the gene dosage level of each patient. Top: Allele-specific gene dosage levels. Note that the gene dosage level of 1 parental allele (green line) is lower than that of the other parental allele (red line), indicating hemizygous deletion of this region. A vertical arrow above the chromosomal panel indicates the location of the *ATM* gene, one of the commonly deleted regions. The first patient had a slight deletion of 11q that also was detected as hemizygous deletion of *ATM1* in 14% cells by fluorescence in situ hybridization (see text). The bottom line schematically displays genes in a second commonly deleted region on 11q. Each horizontal arrow indicates the direction and size of each of the 6 genes involved in this second commonly deleted region of 11q.

formed on the same samples identified 26 of those 33 samples (78%) (Fig. 1) (Table 1). Seven samples that had 13q14 deletion detected by FISH, but not by SNP-chip analysis, had an average of 15% cells (range, 10%-25%) with deletion of 13q14.

Furthermore, to validate the SNP-chip data, we measured allelic dosage levels by real-time PCR (Fig. 3). We used the 2p12 region as an internal control, because it was not involved in any of the abnormalities in our study. The data demonstrated that the region involved in 13q14 deletions detected by SNP-chip analysis had low allelic dosage, but the regions that were not involved in 13q14 deletion possessed intact levels of allelic dosage (Fig. 3, bottom). Only a representative example is shown in Figure 3.

Novel Copy Number Changes

Four common genetic abnormalities, including trisomy 12 (4 patients), deletion of *TP53* (17p13) (3 patients), deletion of *ATM* (11q22) (6 cases), and deletion of 13q14 (26 patients) were identified, as discussed above. All 6 samples that had *ATM* deletion also had other genetic abnormalities, including deletions of 13q14 and 17p13, detected by SNP-chip/FISH analysis (Fig. 1). In 5 of these samples with *ATM* deletion, the deleted regions were very large; the sixth sample (Patient 2) had 2 small deletions very close together (Fig. 2). The first deletion included the *ATM* gene, and the second deletion con-

TABLE 1
Comparison Between Fluorescence in Situ Hybridization and Single Nucleotide Polymorphism Chip Analysis for Detecting 13q Deletions in Chronic Lymphocytic Leukemia

Patient	Percent of cells with Monoallelic/Biallelic loss at 13q by FISH*	Result by SNP Chip†
5	33/21	Loss (H)
6	27/15	Loss
7 (P)	13/—	No loss
8 (P)	43/11	Loss
9 (P)	43/28	Loss (H)
12	14/—	No loss
14	23/3	Loss
16	11/—	No loss
18	10/—	No loss
19	15/7	No loss
20 (P)	65/—	Loss
21	17/—	Loss
22 (P)	52/—	Loss
23	7/53	Loss (H)
24	3/30	Loss
25	45/—	Loss
26 (P)	47/—	Loss
28 (P)	27/49	Loss (H)
30	27/35	Loss (H)
31	66/5	Loss
32	12/—	Loss
38	19/—	Loss
40	38/—	Loss
41 (P)	25/—	No loss
42	20/7	Loss
43	18/—	No loss
44	15/—	Loss
46 (P)	66/8	Loss
47	32/—	Loss
49	24/3	Loss
51	18/—	Loss
52	24/—	Loss
54	25/64	Loss (H)

FISH indicates fluorescence in situ hybridization; SNP, single nucleotide polymorphism; (H), homozygous deletion was detected by SNP-chip analysis; (P), patients with rapidly progressive disease.* The middle column lists the number of cells with either monoallelic or biallelic loss of D13S319 signal on 13q by FISH (— indicates no cells with biallelic loss).
† The right column shows loss of 13q identified by SNP-chip analysis.

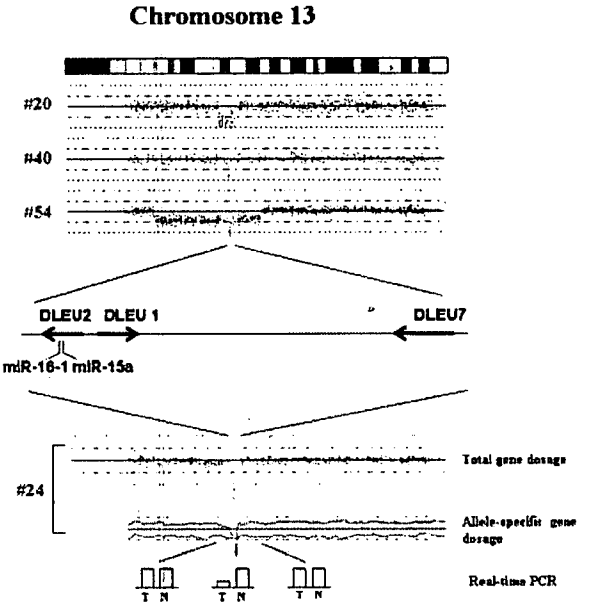

FIGURE 3. Commonly deleted region of 13q14 and whole chromosome 13 uniparental disomy (UPD) with homozygous deletion of 13q14. Top: Representative patients with chronic lymphocytic leukemia (CLL) who had 13q14 deletion detected by single nucleotide polymorphism (SNP)-chip analysis. Individual orange dots represent calculated SNP-chip probe signals, indicating gene dosage levels. The first and second samples show hemizygous deletion of 13q14, and the third sample shows a large hemizygous deletion of 13q and a small homozygous deletion inside of the hemizygous deletion. Middle: Genes in the commonly deleted region of 13q14 are illustrated schematically. Horizontal arrows indicate the direction of transcription and the size of each gene. Two micro-RNAs, miR-15a and miR-16-1, are in intron 4 of the *DLEU2* gene. Bottom: Whole chromosome 13 UPD is shown. Red/green lines represent allele-specific gene dosage. Allele-specific gene dosage lines show loss of 1 parental chromosome (green line) and duplication of the other (red line). Duplicated alleles (red line) have deletion of 13q14 (arrow) leading to homozygous deletion of this region. Each graph shows the allelic dosage levels of 13q14.3 (commonly deleted region), 13q14.1 (centromeric), and 13q21.1 (telomeric) in CLL and normal cells measured by real-time polymerase chain reaction (PCR). T indicates tumor cells; N, reference DNA from a normal, healthy volunteer.

tained 6 other genes (*POU2AF1*, *BTG4*, *FLJ46266*, *LAYN*, *SNFLK2*, and *PPP2R1B*) (Fig. 2). This second commonly deleted region on chromosome 11q was deleted in all 6 samples.

Similar to our findings with *ATM* deletions, all 3 samples that had a 17p deletion had additional genetic abnormalities (Fig. 1). Trisomy 12 was the sole abnormality in all 4 samples as demonstrated by SNP-chip analysis (Fig. 1).

Except for the above-described recurrent abnormalities, the vast majority of genomic changes that have not been described previously were identified by our SNP-chip analysis. Twenty-five samples (45%) had a total of 45 copy number abnormalities other than 13q14 deletion, 11q deletion, 17p deletion, and trisomy 12 identified in SNP-chip analysis (Tables 2, 3).

Of the additional changes that were identified in the SNP-chip analysis, 25 changes were either large deletions (14 samples), duplications (4 samples), UPD (4 samples), trisomy (2 samples), or monosomy (1 sample) that contained >50 genes (Table 2). In addition, 20 changes were either small deletions (13 samples) or duplications (7 samples) and often contained as few as 1 gene or as many as 44 genes

TABLE 2
Single Nucleotide Polymorphism Chip Analysis: Large Copy Number Changes in Chronic Lymphocytic Leukemia*

Chromosomal region	Patient no.	Type of abnormality	Base pair localization
1q32.3-q42	29	Del	208,481,195-227,717,345
4p14-pter	20	Del	pter-34,979,810
4p13-p14	20	Del	40,684,216-44,307,737
5q14.2-q23.2	8	Del	81,990,043-125,733,062
5q14.3-q31.3	29	Del	90,287,988-130,387,114
5q31.3-q33.2	29	Del	143,517,709-154,316,746
5q33.3-q34	29	Del	159,203,291-165,777,302
6q14-q23.2	4	Del	80,810,590-133,976,522
6q16.1-q22.1	30	Del	95,629,083-117,659,576
6q22.33-qter	15	Del	127,493,358-qter
8p12-pter	15	Del	pter-32632781
9q21.11-qter	29	Del	69,208,391-qter
11p14.3-p12	31	Del	25,735,615-35,446,467
11p15.1-pter	35	UPD	pter-19,040,053
Chromosome 13	23, 24	UPD	
17q21.32-qter	12	Dup	42,719,806-qter
17p11.2-pter	48	UPD	pter-21,950,207
Monosomy 21	24		
Trisomy 22	5		
22q11.23-qter	9	Dup	32,159,222-qter
Trisomy X	22		
Xq21.31-pter	15	Del	pter-88,615,115
Xp11.21-pter	29	Del	pter-55,661,160
Xq12-qter	29	Dup	65,546,625-qter

* Large copy number changes other than 11q−, +12, 13q−, and 17p− detected by the single nucleotide polymorphism chip. The table lists deletions (Del), duplications (Dup), uniparental disomy (UPD), trisomy, monosomy, and base pair locations.

(Table 3). Overlapping deletions were detected on 5q, 6q, and Xp (Fig. 4). Two samples had deletion of 5q, and 2 samples had deletion of Xp, as shown in Figure 3A. Four samples had 6q deletions at 6q21 (Fig. 3B). Small alterations that were detected by the SNP-chip analysis involved genes that could be associated with the development of CLL (Table 3). Because only 1 gene, *AIM1*, was involved in the deletion of 6q21 (Fig. 3B), we examined all coding exons and the methylation status of this gene in the 4 samples with deletion of 6q; we observed neither point mutations nor methylation of this gene in these samples (data not shown).

CDR on 13q and UPD

The CDR of 13q14 was localized previously to a 300-kilobase (kb)-long interval on 13q14.2 through 14.3.[18] The CDR in our samples, as identified by SNP-chip analysis, spanned a region of approximately 350 kb that contained this CDR (Figs. 1, 3). Figure 3 shows representative samples of 13q14 deletions. Recently, frequent deletion or mutation of 2 micro-RNAs, miR-15a and miR-16-1, in this region have been reported in CLL.[9,10] All of our samples with 13q− contained these 2 micro-RNAs as a CDR. In our SNP-chip analysis, 6 samples demonstrated homozygous deletion of the 13q14 region (Fig. 3 and data not shown). FISH analysis revealed that these 6 samples had >20% of cells with biallelic loss of 13q14 (Table 1). The presence of cells with biallelic loss of this region

TABLE 3
Single Nucleotide Polymorphism Chip Analysis: Small Copy Number Changes in Chronic Lymphocytic Leukemia*

Chromosomal region	Patient no.	Del/Dup	BP localization	No. of genes	Potential target genes
1q23.2-q23.3	26	Del	156,937, 948-157,642,778	16	
1q32.1	9	Del	199,921,145-200,239,831	7	*BTG2*
1p36.11	10	Del	26,042,344-23,056,134	41	*CD52*
1q42.2-q42.3	2	Del	230,852,980-231,417,785	2	*IRF2BP2*
2p22.2-p22.1	55	Del	37,169,037-39,532,146	14	*SOS1*
4q34.1	40	Dup	175,786,683-176,935,240	2	*ADAM29*
4q35.2	45	Dup	188,796,058-190,012,617	3	*ZFP42*
6q21	15, 28	Del	107,003,343-107,132,119	1	*AIM1*
7q32.1-q32.3	10	Del	128,719,303-129,992,732	13	
9p22.3-p22.2	6	Dup	16,279,143-17,104,199	1	*BNC2*
10q22.1-q22.2	3	Del	72,697,898-72,223,192	44	
10q23.31	3	Del	90,526,429-91,254,269	10	*FAS*
10q23.3	20	Dup	92,020,599-92,812,916	3	*ANKARD1*
12p12.3	24	Del	14,675,168-14,981,176	7	*H2AFJ*
15p13.2-p13.3	8	Dup	28,069,811-30,756,749	5	*KLF13*
15q15.3	6	Del	41,676,268-42,010,479	11	*ELL3*
17q21.31	35	Dup	44,640,555-45,267,454	8	*WNT3*
17q11.2	2	Del	25,744,867-27,046,466	13	*NF1*
20q13.13	53	Dup	45,666,937-46,358,010	1	*PREX1*

Del indicates deletion; Dup, duplication; BP, base pair.
* Small copy number changes that involved <50 genes are listed. Candidate target genes are shown in the far right column.

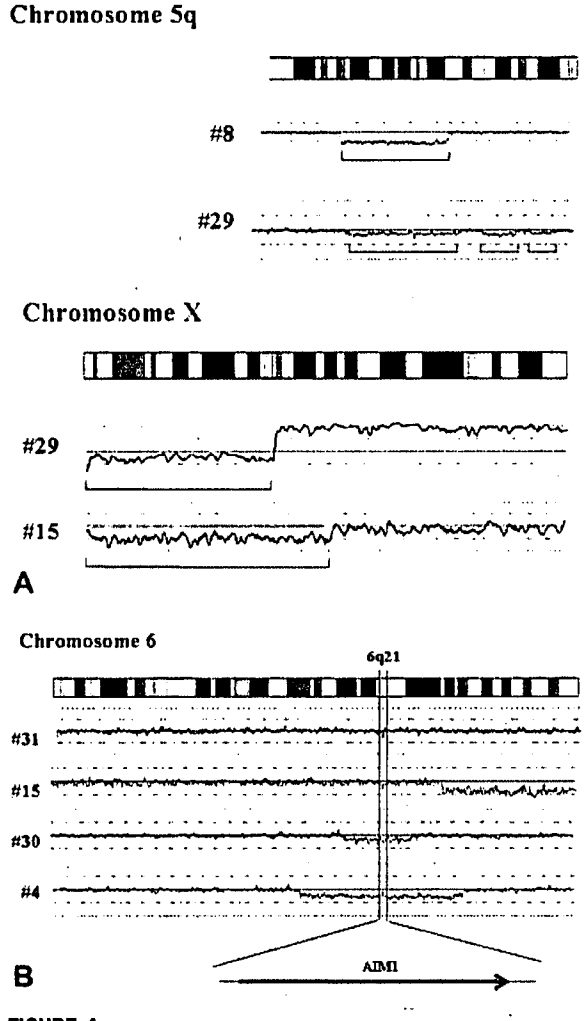

FIGURE 4. Recurrent deletions of 5q, Xp, and 6q detected by single nucleotide polymorphism (SNP)-chip analysis. (A) Deletions of 5q and Xp were detected in 2 patients, respectively, as indicated by brackets. (B) SNP-chip data from 4 samples of chronic lymphocytic leukemia with deletion of 6q. The commonly deleted region is at 6q21 and involves only 1 gene, *AIM1*. A horizontal line at the bottom indicates the direction of transcription of the *AIM1* gene. Each line indicates the gene dosage level of each patient.

was detected in 13 samples, including these 6 samples, by FISH analysis (Table 1).

Unlike comparative genomic hybridization, SNP-chip analysis can detect regions of loss of heterozygosity without copy number changes, so-called UPD.[13] Four of 56 CLL samples had UPD. It is noteworthy that 2 samples with homozygous deletion of 13q14 demonstrated whole chromosome 13 UPD (Table 2) (Fig. 3).

Of the other 2 UPD regions, 1 was located at 11p (11p15.1-pter), and the other was located at 17p (17p11.2-pter), spanning the *TP53* gene (Table 2). Because UPD often is associated with mutations, we sequenced the *TP53* gene at exons 4, 5, 6, 7, and 8 (hotspots of mutations). Codon 72 of *TP53* was arginine (72R) rather than proline (72P) in this instance; this is a polymorphic site (data not shown).

Correlation Analysis of Genetic Abnormalities and Clinical Course

We also examined ZAP-70 expression levels and hypermutation of the *IgVH* gene. Among our 51 patients with early-stage CLL, 19 patients were positive for ZAP-70, and 17 patients had no hypermutation in *IgVH*. Data on the clinical course were available for 51 patients. Nine patients progressed to stage B, 2 patients progressed to stage C, and 3 additional patients began chemotherapy as they progressed clinically (lymphocyte doubling time was <12 months), although they did not fulfill the criteria for stage B. The characteristics of these patients are shown in Table 4. Five of 14 patients had either *ATM* and/or *TP53* deletions, 5 patients had somatic hypermutation of *IgVH*, 8 patients were positive for ZAP-70, and 6 patients were negative for ZAP-70. Even in this small cohort of rapidly progressing patients, deletions of *TP53*, nonmutational status of *IgVH*, and ZAP-70 expression were associated significantly with rapid disease progression (Table 5). Additional genomic abnormalities other than the 4 common ones were not found to be associated significantly with worsening of the disease in our patients (Table 5).

We also compared the genomic abnormalities identified by SNP-chip and/or FISH analysis (Table 6) (Supplement Table). Trisomy 12 and deletion of 13q14 were significantly exclusive ($P = .01$). Deletion of *TP53* (17p13) was associated significantly with the presence of additional genetic abnormalities other than the 4 common genetic abnormalities ($P = .034$). The presence of 13q14 deletion was associated with the absence of additional abnormality ($P = .046$). We compared ZAP-70 expression and *IgVH* mutational status with genomic abnormalities (Supplement Table). ZAP-70 positivity was correlated with nonmutated status of *IgVH* ($P < .001$). Trisomy 12, deletion of 11q22, and deletion of 13q14 were correlated with nonhypermutation of *IgVH* ($P = .033$, $P = .027$, and $P = .027$, respectively) (see Supplement Table). Deletion of 11q22 was correlated with positive ZAP-70 expression ($P = .05$) (Supplement Table).

DISCUSSION

In our 56 samples of early-stage CLL samples, only 10 sample showed no genetic abnormalities by either

TABLE 4
Characteristics of Patients With Progressive Disease

Patient no.	Status*	Age, y	Sex	FISH†	Additional abnormality	IgVH	ZAP-70	Karyotype‡
2	At	86	M	17p−, 11q−	Del 17q11.2	−	−	N
9	At	73	M	11q−	Del 1q32.1 Dup 22q11.23−qter	−	+	N
13	At	66	M	13q−	—	+	+	−Y
7	B	53	M	13q−	—	−	+	N
8	B	79	M	13q−	—	+	−	N
10	B	82	M	13q−	—	−	−	N
17	B	58	M	12+	—	−	+	+12
20	B	66	W	13q−,17p−	Del 4p14-pter Del 4p13-p14 Dup 10q23.3	+	−	ND
22	B	65	W	13q−	Trisomy X	+	−	N
26	B	51	W	11q−	Del 1q23.2-q23.3	−	−	Add(11)(q13)
28	C	81	M	13q−	—	−	+	Del (11)(q22)
29	C	64	W	17p−	Del 1q32.3-q42 Del 5q14.3-q31.3 Del 5q31.3-q33.2 Del 5q33.3-q34 Del 9q21.11-qter Del Xp11.21-pter Dup Xq12-qter	+	+	Iso(X)(q)
41	B	70	W	13q−	—	−	+	N
46	B	82	M	13q−	—	−	+	Complex

FISH indicates fluorescence in situ hybridization; IgVH, immunoglobulin heavy-chain; M, man; Del, deletion; −, absence; +, presence; Dup, duplicate; W, woman; Add, addition.

* At, therapy initiated but still in stage A; B, progression to stage B; C, progression to stage C.

† FISH analysis examined deletions of 11q22 (*ATM*), 17p13 (*TP53*), 13q14, and trisomy 12.

‡ N, normal karyotype, ND, not determined; Complex, complex abnormalities of karyotype. This column describes chromosomal abnormalities (details of karyotypes are shown in Supplement Table 1).

SNP-chip or FISH analysis. The data suggest that genetic abnormalities, including gain, loss, and UPD of genetic materials, frequently occur at an early stage of CLL. In addition to well-documented common genetic abnormalities, including trisomy 12, deletions of *ATM* (11q22), *TP53* (17p13), and 13q14 in CLL, we observed that deletions of 5q, 6q, and Xp were frequent in early-stage CLL. We examined the *AIM1* gene as a target of this deletion. However, neither genetic nor epigenetic abnormalities of this gene were observed in the remaining intact allele. Haploinsufficiency of this gene may be sufficient to contribute to leukemogenesis. Haploinsufficiency of some tumor suppressor genes reportedly suffices to contribute to caricinogenesis.[19] Deletion of 11q is very large, and several genes are deleted in many patients. However, it is believed that the *ATM* gene is the target gene of this deletion.[20] We observed a second commonly deleted region telomeric to the *ATM* gene. This region may contain another tumor suppressor gene associated with the development of CLL. Concurrent deletion of *ATM* and a tumor suppressor gene in this second region may contribute to a poor prognosis for patients with CLL similar to our Patients 2, 9, and 26, who had progressive disease.

In this study, we also analyzed expression levels of ZAP-70 and the mutational status of *IgVH*. We demonstrated for the first time that ZAP-70 expression levels were correlated with 11q22 deletion in early-stage CLL. Although the number of patients was small, we observed that nonhypermutation of *IgVH* was correlated with trisomy 12, deletion of 11q22, and 13q14 in early-stage CLL.

In the current study, we compared data from SNP-chip analysis with data from FISH analysis on several well documented hotspots of deletion, including *TP53*, *ATM*, and 13q14. The sensitivity of FISH analysis was better than that of our SNP-chip analysis at the 13q14 site only when a very minor subclone had the small deletion. In contrast, when a deleted region was large, SNP-chip clearly was able to detect the deletion of 11q22 (*ATM*), even if the clone with this abnormality was not predominant (Fig. 2). We used a 50-k SNP-chip, and this chip had 6 SNP probes encompassing the CDR on 13q14. Now, higher resolution SNP-chips (250-500 k chips) are available and have >30 probes in this region.